

Pressure effects on the magnetoresistance in doped manganese perovskites

H. Y. Hwang

AT&T Bell Laboratories, Murray Hill, New Jersey 07974

and Joseph Henry Laboratories of Physics, Princeton University, Princeton, New Jersey 08544

T. T. M. Palstra, S-W. Cheong, and B. Batlogg

AT&T Bell Laboratories, Murray Hill, New Jersey 07974

(Received 12 July 1995)

We present a detailed study on the effects of applied hydrostatic pressure on the magnetoresistance in doped LaMnO_3 at fixed doping level. In all cases, the application of external pressure monotonically increases the Curie temperature. This is compared with the application of "internal" pressure, which is varied by substituting different rare-earth ions for La. Both effects can be understood in one simple picture that relates the structural modifications to the variation of the Mn-Mn electronic transfer integral. Thus a general phase diagram has been derived with the transfer integral as the implicit microscopic parameter dominating the magnetic and transport properties of doped LaMnO_3 .

The continually increasing demand for magnetic information storage and retrieval has driven a significant worldwide effort to improve the performance of relevant hardware components. A recent success has been the development of magnetic multilayers with giant magnetoresistance for magnetic reading heads.¹ The increased sensitivity of these magnetic multilayers over conventional inductive or permalloy reading heads allows for much higher storage densities. Currently, doped LaMnO_3 is being reexamined as a possible next generation magnetoresistance sensor material.²⁻⁷ These compounds exhibit a very large magnetoresistance in a temperature window around the ferromagnetic ordering of manganese spins. It has recently been established that this temperature window is also associated with a first-order metal-insulator transition, and it is extremely sensitive to lattice strain in the form of chemical pressure, which is varied by substituting different rare-earth ions for La.⁸ Here we report the ability to tune this temperature window by the application of external hydrostatic pressure. By studying the effects in bulk materials, we have uncovered an important aspect of the wide variation in magnetoresistance reported in thin films: the strain induced by substrate lattice mismatch. The structural response due to external pressure (hydrostatic) and internal pressure (ion size mismatch) leads to a modification of the Mn-Mn electronic transfer integral b , which is the important underlying parameter. Therefore the results of these two different forms of strain can be unified in a simple phase diagram. This understanding leads to the ability to simply engineer the magnetoresistance within the constraints of the underlying physical process.

The unique coupling between magnetism and charge transport observed in the doped manganese perovskites originates in the magnetic interaction between Mn^{+3} and Mn^{+4} via "double exchange".⁹ This interaction is mediated by the motion of an electron between the two partially filled d shells with strong on-site Hund's coupling. Several studies have shown that the magnitude and temperature range of significant magnetoresistance are optimized when $\sim 30\%$ of the Mn^{+3} are converted to Mn^{+4} (e.g., by substituting diva-

lent ions for La^{+3} in LaMnO_3).^{2,6} However, this doping level can be realized in a variety of ways that lead to vastly different magnetic ordering temperatures and magnetoresistance properties. Since many of the recent studies have been performed on thin films, the added complications of film growth and formation, substrate lattice mismatch, oxygen deficiencies, etc. have hindered the proper interpretation of these variations.

In order to study the effects of strain on the magnetoresistance, we have prepared polycrystalline samples with the $\text{Mn}^{+3}/\text{Mn}^{+4}$ ratio fixed at $7/3$ but using different rare-earth and alkali-earth ions, and we have studied the effects of applying external pressure. Samples of the family $A_{0.7}A'_{0.3}\text{MnO}_3$ (A is a trivalent rare-earth ion and A' is a divalent alkali-earth ion) have been synthesized through conventional solid-state reaction processing in air. Powder x-ray diffraction showed clean single-phase patterns. The oxygen content was found to be unaffected by various heat treatments (annealing in 200 bars oxygen at 650°C , quenching from 1400°C in air), and chemical analysis and iodometric titration on similarly prepared samples show stoichiometric oxygen content.¹⁰ The resistivity was measured using the standard four-probe technique, and magnetization was measured using a commercial magnetometer (Quantum Design). Hydrostatic pressure was applied in a self-clamping cell using mineral oil as the pressure transmitting medium.¹¹

The temperature-dependent resistivity in earth magnetic field [$\rho_0(T)$] for $\text{Pr}_{0.7}\text{Ca}_{0.3}\text{MnO}_3$ is given on a logarithmic scale in the top panel of Fig. 1 for 1 bar and 5, 10, and 15 kbar applied pressure. The curves are identified by the pressure at room temperature, and this pressure decreases slightly in a reversible and known way at lower temperature.¹¹ The resistivity in 1 bar and 5 kbar is insulating to low temperatures (the resistivity grew too large to be measured below 50 K, but it remained above $10^8 \Omega \text{ cm}$ down to 5 K). The resistivity at 10 kbar, however, exhibits a metal-insulator transition at ~ 80 K, and at 15 kbar $T_{\text{MI}} \sim 100$ K. [Here we have defined T_{MI} as the maximum in $d \ln(\rho)/dT$.] Thus between 5 and 10 kbar $dT_{\text{MI}}/dP \geq 16$ K/kbar (this value is calculated

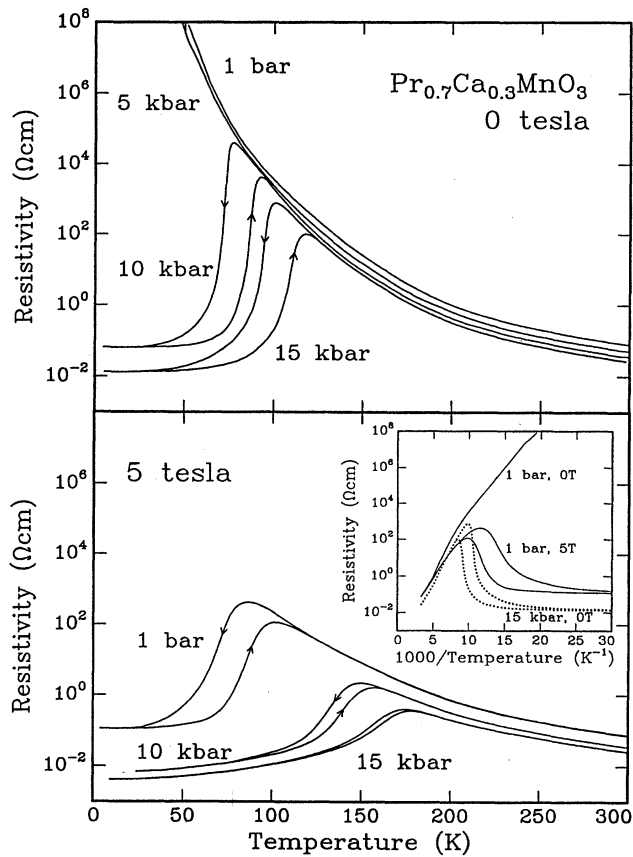


FIG. 1. The large pressure and magnetic-field sensitivity of the temperature-dependent resistivity for $\text{Pr}_{0.7}\text{Ca}_{0.3}\text{MnO}_3$. In the top panel, the resistivity is displayed on a logarithmic scale for 1 bar and 5, 10, and 15 kbar applied pressure in earth magnetic field. In the bottom panel, the resistivity is displayed on a logarithmic scale for 1 bar, 10, and 15 kbar applied pressure in 5 T field. The inset compares the effects of applying pressure and magnetic field separately by examining the resistivity on a logarithmic scale versus $1000/T$.

from the true pressure at T_{MI} , not at room temperature). The strong temperature hysteresis observed at the metal-insulator transition indicates that this is a first-order transition.

In 5 T magnetic field, the temperature-dependent resistivity for 1 bar, 10, and 15 kbar is given in the bottom panel of Fig. 1. As in 0 T, T_{MI} is hysteretic in temperature and increases with increasing pressure. These data are consistent with the notion of a stabilization of the ferromagnetic, low-temperature metallic state by an external field. The transition in 5 T is shifted to higher temperature than that in 0 T. The inset emphasizes the remarkable effect of applying a magnetic field at ambient pressure: the resistivity drops by over eight orders of magnitude in a 5 T field. We also note the similarity of applying pressure and a magnetic field by showing the resistivity in earth magnetic field at 15 kbar applied pressure.

The strong pressure dependence of T_{MI} in both 0 and 5 T is accompanied by an extremely large change in the magnetoresistance as a function of pressure. The magnetoresistance, defined as $(\rho_{0\text{T}} - \rho_{5\text{T}})/\rho_{5\text{T}}$ is shown in Fig. 2 for

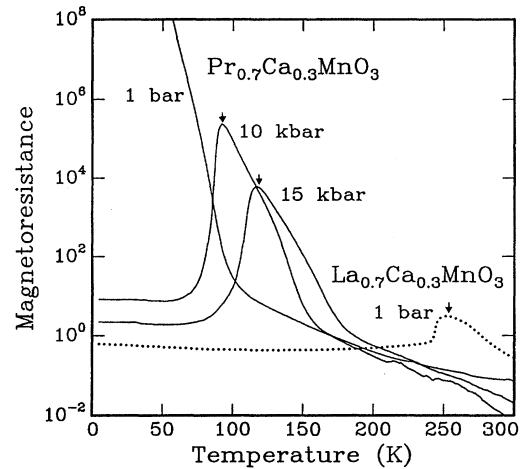


FIG. 2. The dramatic change of the magnetoresistance with both applied hydrostatic pressure and internally generated chemical pressure. The magnetoresistance, defined as $(\rho_{0\text{T}} - \rho_{5\text{T}})/\rho_{5\text{T}}$ is most significant over a narrow temperature window. In $\text{Pr}_{0.7}\text{Ca}_{0.3}\text{MnO}_3$, this temperature window is shifted up with applied pressure, while the magnitude of the magnetoresistance decreases. Consistent with this trend is the magnetoresistance of $\text{La}_{0.7}\text{Ca}_{0.3}\text{MnO}_3$, with the chemical pressure generated by replacing Pr by the larger La. The peak in the magnetoresistance correlates well with the peak in the resistivity in 0 T, which is denoted by the arrows. These data were taken while warming.

$\text{Pr}_{0.7}\text{Ca}_{0.3}\text{MnO}_3$ at 1 bar, 10, and 15 kbar for data taken while warming. The temperature for the maximum magnetoresistance correlates well with the peak in $\rho_{0\text{T}}$ (shown in arrows). As this peak temperature decreases, the magnitude of the magnetoresistance increases dramatically. This can be understood simply from Fig. 1: the magnetoresistance involves a switching from a generic metallic state to a nonmetallic state, and the difference in resistivity between the two states increases with decreasing temperature.

Also shown in Fig. 2 is the magnetoresistance of $\text{La}_{0.7}\text{Ca}_{0.3}\text{MnO}_3$ at ambient pressure. Whereas hydrostatic pressure increases T_{MI} , chemical pressure by substituting La by the smaller Pr suppresses T_{MI} . This may appear counter-intuitive if one only considers changes in the unit-cell volume, but these results can be understood in a straightforward way by carefully considering how the Mn-O-Mn bond angles and distances change as a function of internal and external pressure. These are the structural variations that change the electronic matrix element b describing electron hopping from Mn site to Mn site. We will discuss this point in more detail, since it is central to the understanding of the unified phase diagram.

In the perovskite LaMnO_3 , the manganese ions occupy the B site and are surrounded by oxygen octahedra which share corners to form a three-dimensional network, while the La ions occupy the A site between these octahedra. Electronic conduction involves charge motion between the manganese d orbitals and the oxygen p orbitals, and b , the p - d overlap, is quite sensitive to changes in geometry (bond angle, bond length) brought about by variations in the size of the A-site ions or by externally applied pressure. The origin of the internal chemical pressure is in the size mismatch that

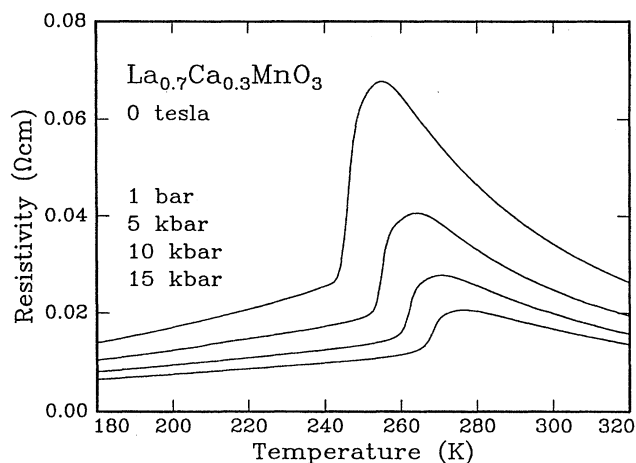


FIG. 3. The pressure dependence of the resistivity for $\text{La}_{0.7}\text{Ca}_{0.3}\text{MnO}_3$ in earth magnetic field on a linear scale, showing the increase in T_{MI} with applied pressure. There was no visible temperature hysteresis for this sample.

occurs when the A -site ions are too small to fill the space in the three-dimensional network of MnO_6 octahedra. For a perfect match, the Mn-O-Mn bond angle θ is 180° . Rather than a simple contraction of bond distances, the smaller A -site ions cause the octahedra to rotate and reduce the excess space around the A -site, resulting in $\theta < 180^\circ$. With decreasing θ , b is reduced. Previous work established this relationship between a decrease in the average ionic radius of the A site $\langle r_A \rangle$ with a decrease in θ , a reduction of b , and therefore a reduction of the Curie temperature T_C .⁸ This structural response is characteristic of perovskites and has been well studied in many compound families such as $R\text{FeO}_3$ and $R\text{NiO}_3$ (R =rare earths).¹²⁻¹⁴

The structural response to external pressure may be less obvious. In the pseudo-perovskite RO_3 , the A site is vacant and the application of pressure causes a spectacular increase in the rotation of the rigid RO_6 octahedra.¹⁵ In the perovskite, however, the A -site ion prevents this collapse, and the application of pressure decreases the rotation through a reduction of the ionic size mismatch. This may be seen as the result of more dense packing of the oxygen ions around the A -site ion. This scenario was proposed in a pressure study of the metal-insulator transition in PrNiO_3 and demonstrated recently by neutron crystallography under pressure.^{16,17} Since the NiO_6 octahedra are less rotated when pressure is applied, θ tends towards 180° and the Ni-O bond is compressed. Therefore both applying external pressure and increasing $\langle r_A \rangle$ lead to an increase of b because both change the relevant geometric structural parameters in the same way.¹⁸

Guided by the realization that the important electronic parameter modified by external and internal pressure is b , we now develop a general and unifying map of the influence of strain on T_C and the associated magnetoresistance. In order to connect this study in hydrostatic pressure with previous work in chemical pressure, and to avoid complications due to different hole concentrations, we examine the particular case of the $\text{Mn}^{3+}/\text{Mn}^{4+}$ ratio fixed at $7/3$. In Fig. 3, the pressure dependence of the resistivity for $\text{La}_{0.7}\text{Ca}_{0.3}\text{MnO}_3$ is shown,

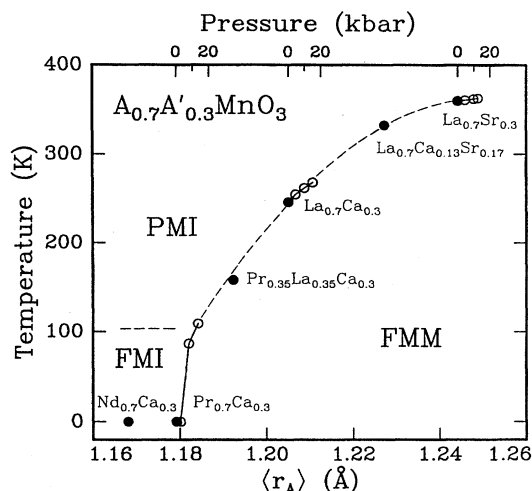


FIG. 4. The phase diagram of $A_{0.7}A'_{0.3}\text{MnO}_3$ as a function of the electronic transfer integral b , which has been varied both by internal and external pressure. Closed circles represent variations of b due to internal pressure (variations of the average A -site ionic radius $\langle r_A \rangle$), and open circles indicate variations of b due to externally applied pressure. The top and bottom axes are closely related in that both increasing $\langle r_A \rangle$ and external pressure straighten out the Mn-O-Mn bond angle closer to 180° , therefore increasing the key electronic parameter b . The pressure data for $\text{La}_{0.7}\text{Sr}_{0.3}\text{MnO}_3$ are from Ref. 20. These data were taken while warming.

which is in good agreement with results for $\text{La}_{2/3}\text{Ca}_{1/3}\text{MnO}_3$ studied by Neumeier *et al.*¹⁹ $\text{La}_{0.7}\text{Sr}_{0.3}\text{MnO}_3$ has recently been examined by Moritomo, Asamitsu, and Tokura.²⁰ We have also examined several different compositions in ambient pressure at regularly spaced intervals of $\langle r_A \rangle$ ($\text{Nd}_{0.7}\text{Ca}_{0.3}\text{MnO}_3$, $\text{La}_{0.35}\text{Pr}_{0.35}\text{Ca}_{0.3}\text{MnO}_3$, and $\text{La}_{0.7}\text{Ca}_{0.13}\text{Sr}_{0.17}\text{MnO}_3$). These results are organized into the phase diagram of Fig. 4 ($\langle r_A \rangle$ is a weighted average calculated from tabulated values²¹). For the samples measured at ambient pressure, the magnetization was also measured, confirming the association of the low-temperature metallic phase with ferromagnetism. For $\text{Nd}_{0.7}\text{Ca}_{0.3}\text{MnO}_3$ and $\text{Pr}_{0.7}\text{Ca}_{0.3}\text{MnO}_3$, however, there was a ferromagnetic transition at 103 K, although the samples appear to be insulating below 5 K.

The application of hydrostatic pressure has a similar effect on T_{MI} as increasing $\langle r_A \rangle$, a result previously observed for the metal-insulator transition in PrNiO_3 .^{16,22} We find that all the applied pressure data can be represented consistently with the ambient pressure data at various $\langle r_A \rangle$ using the same conversion factor of $0.000375 \text{ \AA/kbar}$, relating the bottom and top axes in a unique way. A central result of this work is the observation that increasing b increases T_{MI} , whether it is achieved by chemical doping or external pressure. Thus we find that all of the data can be simply collapsed onto one curve with b as the underlying microscopic parameter.

In summary, this study has demonstrated the large pressure sensitivity of the magnetoresistance in the manganese perovskites. This effect originates in two key microscopic features: the strong coupling between the electronic states and the lattice through the microscopic Mn-O-Mn arrange-

ment, and the strong coupling between charge transport and magnetism through the double exchange interaction. The magnetoresistance is most sensitive to pressure near the low-temperature boundary between metal and insulator. The evolution of T_C with external and internal pressure can be simply mapped onto one another, because both are different

ways of varying the important underlying parameter b , the Mn-Mn electronic hopping parameter. This understanding allows for the engineering and design of manganese perovskites with a range of transition temperatures, a considerable advance towards possible applications of this compound family.

-
- ¹See P. M. Levy, *Science* **256**, 972 (1992), and references therein.
- ²Original work on conducting ferromagnetic properties by G. H. Jonker and J. H. Van Santen, *Physica* **16**, 337 (1950).
- ³C. W. Searle and S. T. Wang, *Can. J. Phys.* **47**, 2703 (1969).
- ⁴R. von Helmholtz, J. Wecker, B. Holzapfel, L. Schultz, and K. Samwer, *Phys. Rev. Lett.* **71**, 2331 (1993).
- ⁵K. Chahara, T. Ohno, M. Kasai, and Y. Kozono, *Appl. Phys. Lett.* **63**, 1990 (1993).
- ⁶Y. Tokura, A. Urushihara, Y. Moritomo, T. Arima, A. Asamitsu, G. Kido, and N. Furukawa, *J. Phys. Soc. Jpn.* **63**, 3931 (1994).
- ⁷S. Jin, T. H. Tiefel, M. McCormack, R. A. Fastnacht, R. Ramesh, and L. H. Chen, *Science* **264**, 413 (1994).
- ⁸H. Y. Hwang, S-W. Cheong, P. G. Radaelli, M. Marezio, and B. Batlogg, *Phys. Rev. Lett.* **75**, 914 (1995).
- ⁹C. Zener, *Phys. Rev.* **82**, 403 (1951); P. W. Anderson and H. Hasegawa, *ibid.* **100**, 675 (1955); P.-G. de Gennes, *ibid.* **118**, 141 (1960).
- ¹⁰Z. Jirák, S. Krupička, Z. Šimša, M. Dlouhá, and S. Vratislav, *J. Magn. Magn. Mater.* **53**, 153 (1985); H. L. Ju, J. Gopalakrishnan, J. L. Peng, Qi Li, G. C. Xiong, T. Venkatesan, and R. L. Greene, *Phys. Rev. B* **51**, 6143 (1995).
- ¹¹J. D. Thompson, *Rev. Sci. Instrum.* **55**, 231 (1984).
- ¹²J. B. Goodenough and J. M. Longo, in *Magnetic and Other Properties of Oxide and Related Compounds*, edited by K. H. Hellwege and A. M. Hellwege, *Landolt-Börnstein*, New Series, Group III, Vol. 4, Pt. a (Springer, Berlin, 1970), p. 126–314.
- ¹³D. Treves, M. Eibschütz, and P. Coppens, *Phys. Lett.* **18**, 216 (1965); G. A. Sawatzky, W. Geertsma, and C. Haas, *J. Magn. Magn. Mater.* **3**, 37 (1976).
- ¹⁴J. B. Torrance, P. Lacorre, A. I. Nazzal, E. J. Ansaldo, and C. Niedermayer, *Phys. Rev. B* **45**, 8209 (1992).
- ¹⁵J.-E. Jorgensen, J. D. Jorgensen, B. Batlogg, J. P. Remeika, and J. D. Axe, *Phys. Rev. B* **33**, 4793 (1986).
- ¹⁶P. C. Canfield, J. D. Thompson, S-W. Cheong, and L. W. Rupp, *Phys. Rev. B* **47**, 12 357 (1993).
- ¹⁷M. Medarde, J. Mesot, P. Lacorre, S. Rosenkranz, P. Fischer, and K. Gobrecht (unpublished).
- ¹⁸The possibility that external pressure might favor the smaller Mn^{+4} over the larger Mn^{+3} , thereby changing the Mn valence, can be limited by the observation that external pressure increases T_{MI} even for compositions for which T_{MI} decreases with increasing $\text{Mn}^{+4}/\text{Mn}^{+3}$ ratio (unpublished).
- ¹⁹J. Neumeier, M. Hundley, J. Thompson, and R. Heffner (unpublished).
- ²⁰Y. Moritomo, A. Asamitsu, and Y. Tokura, *Phys. Rev. B* **51**, 16 491 (1995).
- ²¹R. D. Shannon, *Acta Crystallogr. A* **32**, 751 (1976).
- ²²X. Obradors, L. M. Paulius, M. B. Maple, J. B. Torrance, A. I. Nazzal, J. Fontcuberta, and X. Granados, *Phys. Rev. B* **47**, 12 353 (1993).